Dragoș Andrei POPICA, Sebastian-Marian ZAHARIA

DESIGN, AERODYNAMIC ANALYSIS AND ADDITIVE MANUFACTURING OF A RADIO-CONTROLLED AIRPLANE

Abstract: *Additive manufacturing is a technology used in a wide range of industrial applications, from the digital model to the final physical production and often testing of parts. In this paper a radio-controlled airplane model was designed, analysed in terms of aerodynamic performance, and manufactured using the thermoplastic filament extrusion process. The preliminary aerodynamic analysis resulted in a maximum lift coefficient of about 1 corresponding to a drag coefficient of 0.058. This paper deals with the description of the additive manufacturing procedure of the radio-controlled model components and, finally, the assembly procedure of the whole model. At the end it can be stated that the thermoplastic extrusion process can be successfully used for the manufacture of radio-controlled model airplane or scale model airplane for the purpose of determining aerodynamic performance and conducting tests in wind tunnels or during flight.*

Key words: *RC airplane, fused filament fabrication, design, aerodynamic analysis.*

1. INTRODUCTION

Fused filament fabrication (FFF) or 3D printing refers to the production of three-dimensional parts, starting from a 3D digital model, by overlaying layers of material on a millimetre scale, until the desired part is obtained [1]. The industry is always in a continuous process of development, so with it the FFF process is becoming increasingly popular with applications in various industries (aerospace, automotive, medical, electronics), as well as among hobbyists.

The field of additive manufacturing has been developing recently thus it became inevitable that it would also be used to produce unmanned aerial vehicle [2], [3], some as a hobby, others as prototypes for testing [4]. Radio-controlled airplane can be made from various materials: wood, foam, composite materials and plastics [5], [6].

Unmanned aerial vehicle has been developed to perform military and civilian applications such as: reconnaissance missions, attack missions, rescue missions, wildlife surveillance, border patrol, firefighting, agricultural surveillance or weather data acquisition [5], [6].

The FFF process is used for the manufacture of small unmanned aerial vehicle due to the advantages (elimination of moulds, short manufacturing time, wide range of materials, low cost of 3D printing systems and filaments) that additive processes confer [7]. The manufacture of unmanned aerial vehicle using the FFF process is a field of intense research by universities/research institutes and aviation enthusiasts. Currently, various types of radio-controlled airplane have been 3D prototyped with different aerodynamic configurations.

Starting from the review of the current state of knowledge, it can be highlighted that there are interdisciplinary scientific challenges that can be exploited, generating important results in manufacturing and operating of radio-controlled airplane manufactured by the FFF process. The main goal of the study is the design, preliminary aerodynamic analysis and physically fabricate a radio-controlled airplane manufactured by additive technologies.

2. MODEL DESIGN

For the design of the structural solution, the design of EDGE 540 aerobatic airplane was chosen [8]. Based on this model, two sketches were made to aid 3D modelling using the SolidWorks 2020 software system. Thus, two sketches were made describing the preliminary design of the radio-controlled airplane. Based on these two sketches, 3D modelling was started using the SolidWorks software system.

The next step was to choose the optimal airfoil for an aerobatic airplane. A comparative study was carried out between NACA 2411, NACA 2412, NACA 3312 for the wing, and NACA 0009 for the empennage. The airfoil study was performed in the XFLR5 software system. Next the lift coefficient (Cl) was plotted as function of the drag coefficient Cd (Figure 1).

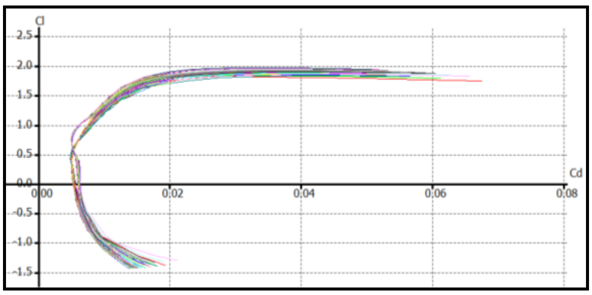

Figure 1 Variation of the lift coefficient as function of the drag coefficient.

This comparative study concludes that a thicker airfoil induces higher lift and drag, resulting in lower speed, while a thinner airfoil induces lower lift and drag, resulting in increased flight speed. Thicker profiles are ideal for gliders. An aerobatic airplane which needs high speed and an airplane made by additive manufacturing processes which is heavier and which needs higher speed led to the choice of the NACA 2411 airfoil.

For the 3D modelling, the scanned sketches will be uploaded into the dedicated software and the shape of the airplane will be modelled with surfaces, drawing the outline of the airplane and some cross sections (Figure 2). The wing and empennage skin is 0.7 mm, while the fuselage skin is 0.8 mm. The wings, fuselage and empennages are all reinforced with carbon fibre pipes and rods.

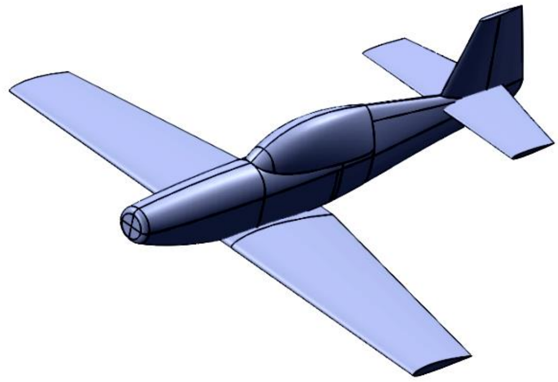

Figure 2 Solid airframe of the model.

The next step was to design the internal structure of the airplane. The structural solution chosen was to use spars reinforced with carbon pipes and rods. Thus, the wing has a main spar, positioned near the centre of pressure, reinforced with a square carbon fibre pipe (10 mm x10 mm x1000 mm) and two secondary spars, one in the leading edge and the other towards the trailing edge, reinforced with 1.2 mm diameter carbon rods (Figure 3). The ailerons are reinforced with a printed spar and a 1.5 mm diameter carbon rod.

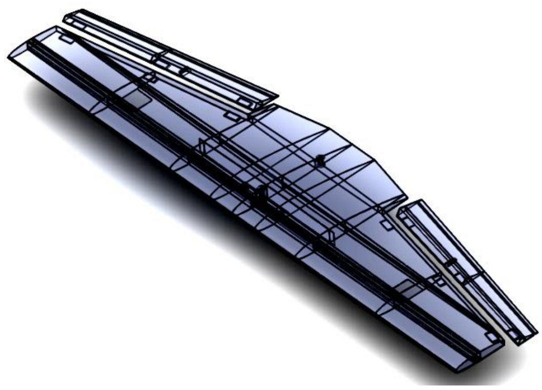

Figure 3 Wing structure.

The horizontal empennage, consisting of the horizontal stabiliser and elevator, has an internal structure also made of spars. The horizontal stabiliser is reinforced with a 6 mm outer diameter carbon pipe, the leading edge has a 1.5 mm carbon rod and towards the elevator there is a 3D printed spar. All 3D printed and non-carbon fibre reinforced spars are 1 mm thick. The elevator consists of a spar, towards the trailing edge, reinforced with a 1.5 mm carbon rod and a main spar made of a 4 mm outer diameter carbon pipe, which help to move the left and right half of the elevator at the same time (Figure 4).

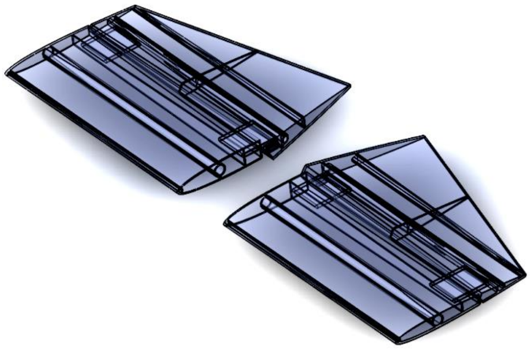

Figure 4 Structure of the horizontal empennage.

The vertical empennage, consisting of the vertical stabiliser and the rudder, is reinforced only with 3D printed spars. The vertical stabiliser also has a 4 mm outer diameter carbon pipe to ensure the proper position of the vertical empennage when assembled with the fuselage, but also for strength (Figure 5).

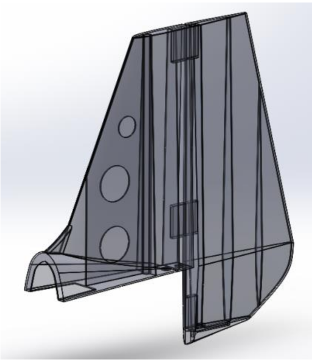

Figure 5 Structure of the vertical empennage.

The fuselage has two 1.5 mm diameter carbon fibre rod reinforced spars, the top and bottom are fitted with 3D printed, non-reinforced spars, and the middle, from the cockpit to the engine, a 2 mm thick resistance plate with lightening holes in it, was also designed to fit the electronic components. The engine will be attached by a 3D printed 3 mm thick frame. The wing will be removable and will be attached to the fuselage with screws in bores provided in both the wing and the fuselage (Figure 6).

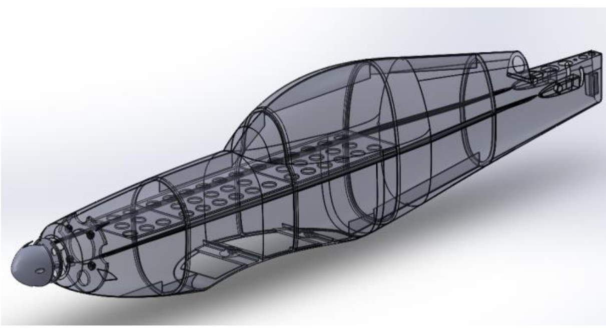

Figure 6 Structure of the fuselage.

In order to be 3D printed, the airplane is divided into sections of maximum 200 mm, as shown in Figure 7.

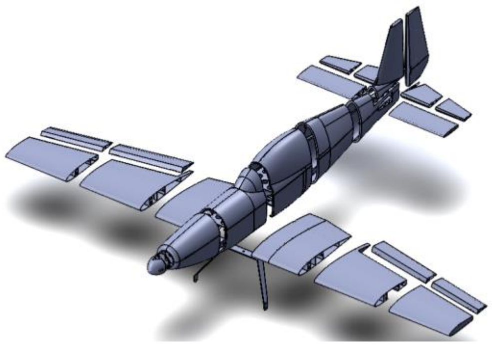

Figure 7 Dividing the plane into sections for 3D printing.

Table 1 shows the characteristics of the radio-controlled airplane designed to be manufactured by the FFF process.

Table 1

Airplane characteristics.

Characteristic	Value
Wing Span	1000 mm
Length	949 mm
Height	300 mm
Weight	1530 g
Root chord	240 mm
Tip chord	140 mm
Airfoil wing	NACA 2411
Airfoil empennage	NACA 0009

Flight mission: this radio-controlled airplane has been designed as an aerobatic airplane, so its main mission is aerobatics, but it can also be used for training those who want to learn radio-controlled flight or even for perfecting aerobatic flight.

The online software eCalc [9] was used to determine the flight performance, where airplane data on geometry, but especially data on electronic and mechanical components were entered (Table 2). Based on the software the thrust-to-weight ratio is of 0.83:1 and the resulting thrust was calculated to be 2.5 kg and the mixed flight time was 5.1 minutes.

Table 2

Electronic and mechanical components of the airplane.

Component	Type
Engine	BL Outrunner A2814/8 D35x36 1000 kV
Propeller	Gemfan Elektro 11 x 7 (APC)
Electronic speed control (ESC)	Brushless Fly Pro 30A
Battery	LiPo TCBWORTH 11.1V/1500mA
RC airplane servo	4 x NANO PS-1109HB 1,9 kg/cm / 0,07s Analog
Transmitter	FrSKY TARANIS X9D PLUS
Receiver	FrSKY X8R

3. PRELIMINARY AERODYNAMIC ANALYSIS OF THE AIRPLANE

Aerodynamic analysis of the airplane will be performed in XFLR5software system. After the analysis of the aerodynamic profiles, the modelling of the airplane is carried out. Three different airplane are defined to obtain separately the polar curves for the wing, the empennage and the whole airplane. First the wing and the empennage are defined, but for this some geometrical parameters and angle of attack need to be set. The wing and the empennage are modelled using some parameters (y-distance between sections, chord of each section, airfoil, dihedral angle and twist angle). The fuselage modelling is done by defining the number of sections and the distance between them.

For the aerodynamic analysis it is necessary to define the airflow velocity (for this case 10 m/s was chosen), the weight of the airplane and the angles of attack α (ranging from -5° to 10°). Thus, the polar curves of the wing, the empennage and the whole airplane were obtained (Figure 8).

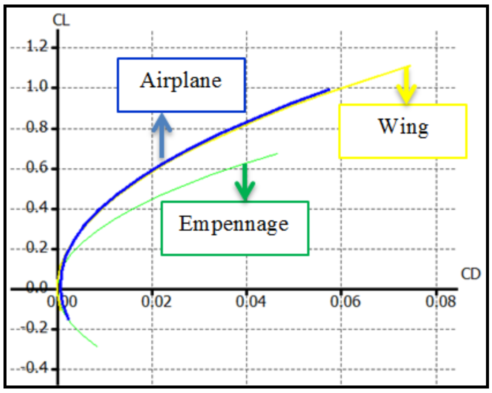

Figure 8 Polar curves of the wing, empennage and the whole airplane.

From the polar of the lift coefficient it can be shown that:

- the airplane has a lift coefficient (Cl=1) and a drag coefficient (Cd=0.058);
- the wing has a lift coefficient Cl=1,1 and a drag coefficient Cd=0,074;
- the empennage has a lift coefficient Cl=0.69 and a drag coefficient Cd=0.046.

Moreover, the distribution of the pressure coefficient (Cp) on the airplane at certain angles of attack was also analysed using aerodynamic analysis (Figure 9).

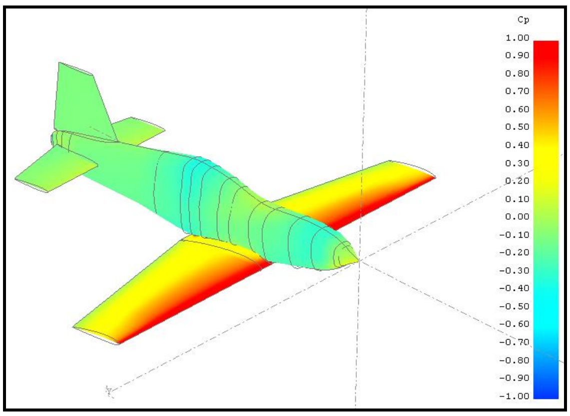

Figure 9 Variation of the pressure coefficient on the whole airplane at 5° angle of attack.

4. FINITE ELEMENT ANALYSIS OF THE WING STRUCTURE

Finite element analysis of the strength structure was carried out on the entire wingspan in the Ansys 16 software. The wing stress (force) was determined by multiplying the following terms: mass airplane (ma=1530 g), gravitational acceleration (g=9.81 m/s^2), safety factor (s=1.5) and load factor (n=2), and the result is 45.03 N. For the finite element analysis the following steps were performed: the wing model was imported; the characteristics of the material from which the airplane is made - polylactic acid (PLA) - were defined; the wing was discretized with 2 mm discretization elements; boundary conditions were applied - fixed was performed in the screw bores, with which the wing will be attached to the fuselage; the calculated force of 45.03 N was applied. The maximum total deformations (1.25 mm) are found at the wingtip and have allowable values for the airplane wingspan of one metre (Figure 10). The maximum equivalent stresses (Figure 11) have values up to 8.22 MPa and they occurred in front of the first attachment point of the wing to the fuselage. It can be concluded that the equivalent stress does not exceed the material compressive and tensile strength, the maximum tensile strength of polylactic acid (PLA) is 54.1 MPa, and the maximum compressive strength is 60.5 MPa. This means that the wing withstands the applied stresses, which are also taken up by the carbon fibre reinforcements.

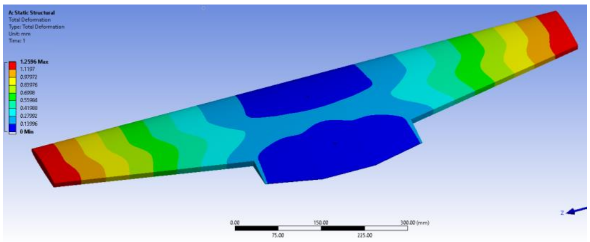

Figure 10 Total deformations.

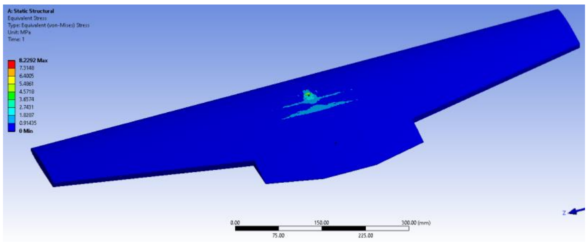

Figure 11 Equivalent stresses.

5. ADDITIVE MANUFACTURING OF RADIO-CONTROLLED MODEL AIRPLANE COMPONENTS

The 3D printer used to build the radio-controlled airplane components was Creality Ender 3. The material used to manufacture the airplane components was polylactic acid (PLA), as it is a low-cost and easy-to-print material that does not require much testing to adjust the optimal parameters before 3D printing.

Table 3

Manufacturing parameters of airplane components.

Parameter	Value
Filament diameter	1.75 mm
Infill density	100%
Print speed	70 mm/s
Travel speed	100 mm/s
Extrusion temperature	205°C
Layer height	0.2 mm
Nozzle diameter	0.4 mm

The preparation for the additive manufacturing of the airplane components (Figure 12) was carried out in the Ultimaker Cura software system, where the manufacturing parameters were established (Table 3).

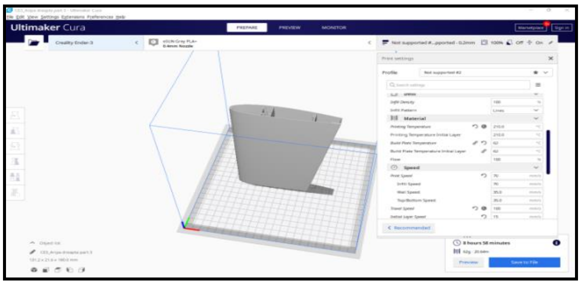

Figure 12 Preparation for manufacturing of a wing section.

Sequences of 3D printing of airplane components are described as follows: 3D printing of a wing section (Figure 13) and 3D printing of a fuselage section (Figure 14).

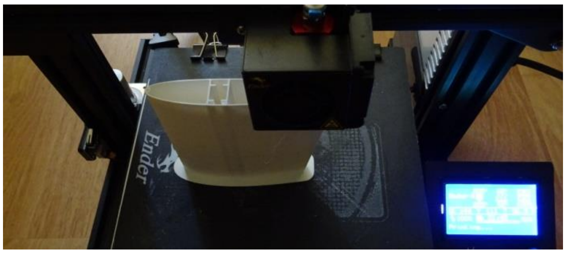

Figure 13 3D printing of a wing section.

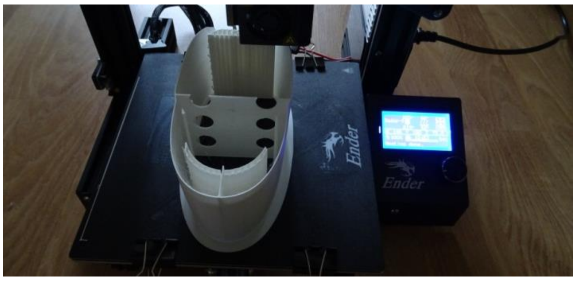

Figure 14 3D printing of a fuselage section.

The manufacture of the components was carried out without any difficulties because all the structures were designed to consider the limitations of the FFF process. In conclusion, the total 3D printing time of the entire airplane was 200 hours, distributed as follows: fuselage sections (Figure 15) were printed in 85 hours; wing sections (Figure 16) were printed in 66 hours;

empennage sections (Figure 17) were produced in 20 hours and the control surface sections were produced in 29 hours.

Figure 15 3D printed fuselage components.

Figure 16 3D printed wing components.

Figure 17 3D printed components of the empennage.

The only part of the airplane that was not manufactured by thermoplastic extrusion is the landing gear. It was decided that the landing gear should not be 3D printed because it needs to be strong and light, so the landing gear was made of composite materials (fibreglass and epoxy resin). The first step was to create a mould of the landing gear, made of wood, and then the fibreglass strips were cut. Ten layers of fibreglass with a density of 100 g/m^3 were used to obtain a landing gear thickness of 1.5 mm. The resin mixture with hardener was prepared with the mixing ratio 100:30 parts, and each impregnated layer was added to the mould (Figure 18). Compression was carried out using plywood strips, and in order for the plywood not to stick to the component, plexiglass strips were added between the plywood strips and the mould.

Figure 18 Manufacturing the landing gear in the mould.

6. ASSEMBLY AND GROUND TESTING OF THE RADIO-CONTROLLED AIRPLANE

The assembly of the radio-controlled airplane was carried out by components: empennage, fuselage, wing and landing gear. The components were assembled by bonding and using a cyanoacrylate adhesive (used mainly for bonding plastics). The airplane was assembled in the following stages:

- Removing the support from each component;
- Finishing and deburring of components;
- Bonding of the wing sections (Figure 19);
- Bonding of the control surface sections;
- Assembly of the empennage and tail landing gear (Figure 20);
- Bonding of the fuselage sections (Figure 21);
- Bonding of servomechanism mounts;
- Assembly of the landing gear;
- Assembly of the control rods;
- Assembly of the electronic equipment (engine, servomechanisms, speed regulator, receiver, battery);
- Final assembly of the radio-controlled airplane (Figure 22).

Figure 19 Assembly of wing sections.

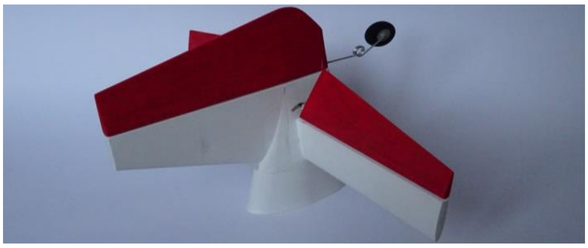

Figure 20 Assembly of fittings and tail landing gear.

Figure 21 Assembly of the fuselage - empennage.

Figure 22 Assembled airplane equipped with electronic components.

At this stage the functioning of the electronic components and controls was checked. In this way, the deflection control and operation of the engine are checked. The ground tests on flight commands consisted of:

- Aileron deflection (left-right);
- Flaps deflection;
- Left-right rudder deflection (Figure 23);
- Up-down depth rudder deflection (Figure 24);
- Checking the engine operation (Figure 25).

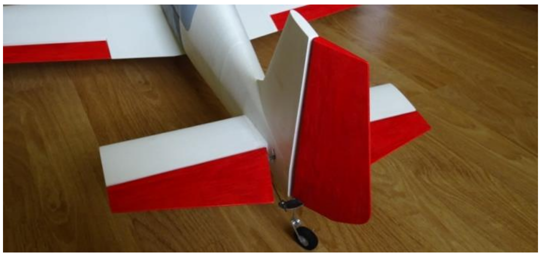

Figure 23 Rudder deflection.

Figure 24 Elevator deflection.

Figure 25 Engine testing and taxiing of the airplane.

7. CONCLUSIONS

In conclusion, applying the FFF process to the manufacture of a radio-controlled airplane, it is a suitable manufacturing process for prototyping. This process is low cost and, more recently, accessible to everyone, as affordable and small 3D printers have recently appeared on the market.

The low manufacturing costs are also due to the fact that moulds are not needed to manufacture the model, which can be very expensive. Another advantage of the FFF process is that it does not require a lot of machining tools, the part is produced within the required parameters, in some cases only requiring the removal of supports from the print or finishing with sandpaper. The FFF process is a versatile manufacturing method and can produce complex parts of various shapes and sizes. The airplane made by the FFF process, fully equipped for flight, has a mass of 1530 grams and falls into the open operations category, operational subcategory A2. Aerodynamic analyses show that the airplane has a lift coefficient of 1 and a drag coefficient of 0.058. Analysing the strength structure of the wing with finite element method, it can be concluded that it resists stresses at a load factor equal to 2. Performance calculations show that the airplane has a maximum speed of 94 km/h, a stall speed of 23 km/h and flies for about 5.1 minutes. This radio-controlled airplane was designed as an aerobatic airplane but can also be used for training those who wish to learn radio-controlled flight.

REFERENCES

[1] Saleh Alghamdi, S., John, S., Roy Choudhury, N., Dutta, N.K. (2021). *Additive Manufacturing of Polymer Materials: Progress, Promise and Challenges*. Polymers, Vol. 13, pp. 1-39, ISSN 2073-4360.

[2] Skawiński, I., Goetzendorf-Grabowski, T. (2019). *FDM 3D printing method utility assessment in small RC airplane design.* Airplane Engineering and Aerospace Technology, Vol. 91, pp. 865–872, ISSN 0002-2667.

[3] Pascariu, I.S., Zaharia, S.M. (2020). *Design and testing of an unmanned aerial vehicle manufactured by fused deposition modeling.* Journal of Aerospace Engineering, Vol. 33, No.4, ISSN 0893-1321.

[4] Goh, G., Agarwala, S., Dikshit, V., Sing, S. and Yeong, W. (2017). *Additive manufacturing in unmanned aerial vehicles (UAVs): Challenges and potential.* Aerospace Science and Technology, Vol. 63, pp. 140–151, ISSN 1270-9638.

[5] Chung, P.-H., Ma, D.-M., Shiau, J.-K. (2019). *Design, Manufacturing, and Flight Testing of an Experimental Flying Wing UAV*. Applied Sciences, Vol. 9, pp. 1-22, ISSN 2076-3417.

[6] Hassanalian, M., Abdelkefi, A. (2017). *Classifications, applications, and design challenges of drones: A review.* Progress in Aerospace Sciences, Vol. 91, pp. 99–131, ISSN 0376-0421.

[7] Najmon, J.C., Raeisi, S., Tovar, A. (2019). *Review of additive manufacturing technologies and applications in the aerospace industry*. In Additive Manufacturing for the Aerospace Industry, Elsevier: Amsterdam, The Netherlands, pp. 7–31.

[8] https://pilot-rc.com/category/acrobatic/edge-540-v3/, *Accessed*: 2023-05-19.

[9] https://www.ecalc.ch/motorcalc.php, *Accessed*: 2023 05-19.

Authors:

Msc. student Dragoş Andrei POPICA, Transilvania University of Braşov, Department of Manufacturing Engineering, E-mail: dragos.popica@student.unitbv.ro

Assoc. prof. Sebastian-Marian ZAHARIA, Transilvania University of Braşov, Department of Manufacturing Engineering

E-mail: zaharia_sebastian@unitbv.ro